CHEMISTRY OF MATERIALS

ARTICLE

pubs.acs.org/cm

Toward Discrete Multilayered Composite Structures: Do Hollow Networks Form in a Polycrystalline Infinite Nanoplane by the Kirkendall Effect?

Firat Güder,[†,*] Yang Yang,[†,*] Silvana Goetze,[‡] Andreas Berger,[‡] Roland Scholz,[‡] Daniel Hiller,[†] Dietrich Hesse,[‡] and Margit Zacharias[†]

[†]Nanotechnology, Institute of Microsystems Engineering, Faculty of Engineering, Albert-Ludwigs-University of Freiburg, Georges-Köhler-Allee 103, D-79110 Freiburg, Germany

[‡]Max Planck Institute of Microstructure Physics, Weinberg 2, D-06120 Halle, Germany

ABSTRACT: Spatial confinement in nanostructures is of critical importance in the fabrication of tubular and hollow spherical objects using void formation via the Kirkendall effect. For both core−shell nanowires and nanospheres, generated vacancies are trapped within an area that is confined either in two (nanowires) or all three (nanospheres) spatial dimensions. When the void formation is extended to multilayered thin films where only one dimension (thickness) is in the nanoscale and the other dimensions are infinitely extended, the final morphology of the formed voids can be significantly different. Using a multilayered system consisting of alternating layers of ZnO and Al_2O_3 grown by atomic layer deposition (ALD), we investigate the effects of annealing temperature, annealing duration, layer thickness, polycrystallinity, grain size, and reaction space on the solid-state diffusion process and final morphology of the produced Kirkendall voids. As opposed to single-crystal ZnO nanowires coated with an amorphous Al_2O_3 shell, which involves only a one-way transfer of ZnO into Al_2O_3, polycrystalline ZnO layers in the multilayered films also cause diffusion of Al_2O_3 into ZnO layers via grain boundary diffusion. Temperature treatment at 700 °C generally yielded layered voids for multilayered films with thin component sublayers. This morphology was well-preserved even at 800 °C. In contrast, partially continuous nanogap morphologies were formed for multilayered films with thick sublayers at 700 °C. However, only interlaced voids were produced at 800 °C in this case, because of grain boundary migration induced oriented attachment. The mechanisms revealed here allow precise fabrication and design of porous multilayered composite films with controlled void morphology.

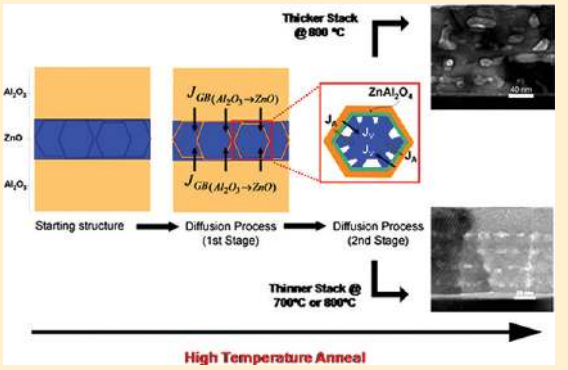

KEYWORDS: multilayered structure, Kirkendall effect, grain boundary diffusion, grain boundary migration, oriented attachment

INTRODUCTION

In recent years, the nanoscale Kirkendall effect has extensively been utilized to produce a variety of hollow nanospheres, nanotubes, hollow/porous hierarchical nanostructures, and even more.[1−7] This fabrication regime involves unequal atomic diffusivities across a binary-phase interface, and is compensated by the injection of lattice vacancies that can accumulate and supersaturate into voids near the interface along the side of the faster diffusing species. Core−shell nanowires/nanospheres have two or all three dimensions at the nanoscale. Injected vacancies in these confined spaces are easy to supersaturate and accumulate into single voids. Consequently, nanotubes and hollow nanospheres can evolve from the initial core−shell nanostructures, exploiting the nanoscale Kirkendall void formation process.

The established knowledge on the interdiffusion behavior of diverse binary thin-film diffusion couples provides a rich database for rational selection and design of core−shell precursors with unequal diffusion coefficients. However, for structures directly derived from film stacking, for example, binary nanoscale multilayered systems with alternating A and B layers, it has not been revealed until now how the Kirkendall void formation is evolved. In contrast to core−shell nanostructures, binary nanoscale multilayered systems have only one dimensional parameter at the nanoscale (the respective layer thickness), whereas the other dimensions are infinitely extended. Besides a large diffusion interface area,[8,9] another distinct feature of the multilayered systems is that film stacks grown by current deposition techniques frequently encounter a polycrystalline structure. The wide network of short circuit diffusion paths composed of grain boundaries (GBs) should play a crucial role during the thermal interdiffusion process.[10] Therefore, the void formation regimes can be significantly different from the core−shell nanowires/nanospheres normally representing an encapsulated single-crystal core.

Received: May 23, 2011
Revised: August 7, 2011
Published: September 22, 2011

By using single-crystal ZnO nanowires coated with an amorphous Al_2O_3 layer, our group has studied the reaction mechanisms and various other factors influencing the thermal diffusion process in ZnO−Al_2O_3 core−shell nanowires in detail.[11−14] It was revealed that the bulk solubility of Al_2O_3 in ZnO is almost zero at elevated temperatures and the solubility of ZnO in Al_2O_3 is very high. This example represents an extreme Kirkendall type diffusion process as it is effectively a one-way outward diffusion of ZnO into Al_2O_3, accompanied by the formation of spinel $ZnAl_2O_4$.

In this article, we extend this thermal diffusion couple and use periodically alternating Al_2O_3 and ZnO layers as a model structure to investigate the unequal interdiffusion process in nanoscale multilayered systems. The intended Al_2O_3/ZnO multilayered structure consists in total of nine alternating layers (five Al_2O_3 and four ZnO) sequentially grown by atomic layer deposition (ALD). The Al_2O_3 layers are amorphous in nature while the ZnO layers are polycrystalline. We explore the possibility of applying the nanoscale Kirkendall effect in a polycrystalline infinite space for the fabrication of discrete $ZnAl_2O_4$ multilayered structures. Depending on the process parameters such as annealing time, reaction temperature, and film thickness, ordered/unordered embedded cavities or partially continuous large gaps are formed. The results indicate that the void morphology in the final spinel $ZnAl_2O_4$ products can be effectively regulated. These findings are further extended to various Al_2O_3/ZnO multilayered 1D nanosystems to instruct the fabrication of complex 1D porous nanostructures. This case study is of particular importance for producing layered compounds and porous thin films derived from Kirkendall-type thin-film diffusion couples, and for increasing the experimental predictability of target nanostructures.

EXPERIMENTAL SECTION

Al_2O_3/ZnO multilayered films, consisting of five layers of Al_2O_3 and four layers ZnO, were deposited by atomic layer deposition at 150 °C (Oxford Instruments, OpAL) on 1% HF treated Si (100) substrates. The thickness of each Al_2O_3 and ZnO layer was precisely controlled by the number of diethylzinc (DEZ)/H_2O and trimethylaluminum (TMA)/H_2O exposure cycles. The pulse length for DEZ and TMA were set to 40 and 20 ms, respectively. After each metalorganic precursor pulse, a 20 ms dose of H_2O was released into the reactor as the oxidant. Before deposition, the reactor was pumped down to 8 mTorr and maintained between 170 and 190 mTorr during the process. N_2 gas was used as the purging agent to remove any residual/byproduct gases to prevent parasitic reactions.

The long time anneals at 700 and 800 °C in air were performed using a standard box furnace manufactured by Carbolite. The short time anneals were performed in a rapid thermal processing furnace (Jipelec JetFirst 200C).

$ZnAl_2O_4$ nanotube templates were fabricated using ZnO/Al_2O_3 core−shell nanowires and annealing them at 800 °C in air. Commercially available multiwall carbon nanofibers were purchased from Nanothinx, Greece. ZnO nanowires were grown via a vapor transport technique on silicon or GaN/sapphire substrates using gold as catalyst. ZnO (Sigma Aldrich 99.999%) and graphite (Alfa/Aesar ∼200 mesh) powders were used as source, mixed in a 1:1 ratio. The substrate was placed near the source powder in a quartz tube furnace. The pressure inside the tube was maintained at 200 mbar using O_2 (0.001 sccm) and Ar (7 sccm) as carrier gases and a growth temperature between 875 and 939 °C was maintained.

The $ZnAl_2O_4$ nanotube templates were coated with a single layer of ZnO (12 nm) and an Al_2O_3 (24 nm). The coated templates were then annealed at 700 °C in air. Carbon nanofibers were coated with a triple layered film stack consisting of a single layer of 12 nm ZnO layer sandwiched between two 24 nm Al_2O_3 layers and the final structure was annealed at again 700 °C in air. And finally, ZnO nanowires with a TiO_2 diffusion barrier shell were coated with a nine layer multilayered film with alternating layers of ZnO (four layers of 12 nm) and Al_2O_3 (five layers of 24 nm) films, which were subsequently annealed at 800 °C.

Cross-sectional TEM samples were prepared by the standard preparation technique. A stack was first made by gluing together two substrate fragments (film-to-film). After the mechanical thinning down process (mechanical polishing), final thinning was done with the help of ion milling. The cross-sectional TEM samples were analyzed using two transmission electron microscopes, viz. a CM20T from Philips (200 kV) and a JEM-4010 from JEOL (400 kV) for high resolution TEM micrographs. A Philips CM20FEG scanning TEM instrument (200 kV) equipped with an EDX detector (IDFix-system, SAMx) was used for energy-dispersive X-ray spectroscopy analysis. 1D nanostructures were observed by a JEOL JEM-1010 electron microscope (100 kV).

RESULTS AND DISCUSSION

Growth of Al_2O_3/ZnO Multilayered Films by ALD. A schematic view of the ALD-grown Al_2O_3/ZnO multilayered films is shown in Figure 1a. ALD, a gas phase deposition technique, has been widely used to produce thin-film structures for various applications. Unlike conventional chemical vapor deposition (CVD), in a typical ALD process, the reaction gases are released into the deposition chamber separately, in a self-limiting and alternating manner. This property of the ALD process ensures precise monolayer thickness control and allows deposition of various high-quality and conformal binary oxides, sulfides, metals and other binary/ternary materials in a wide temperature window.[15−18] In our experiments, Si (100) wafers were selected as the substrate material because no major interdiffusion occurs between the Si substrate and the ALD-deposited Al_2O_3 films at temperatures even as high as 1200 °C.[19] Therefore, the bottom Al_2O_3 layer is a good diffusion barrier to prevent interactions with the underlying substrate. For studying the effects of layer thickness/grain size on the Kirkendall void formation in multilayered films, we prepared two different multilayered samples, namely sample I and sample II, for the subsequent solid-state reactions. For both cases, a thickness ratio of 2:1 for Al_2O_3:ZnO was employed to ensure complete consumption of each ZnO layer in the $ZnAl_2O_4$-forming reaction at high temperatures. Figures 1b, c present a typical cross-sectional transmission electron microscopy (TEM) image of the samples I and II, respectively, in which the dark segments correspond to ZnO and the light ones to Al_2O_3. Sample I consists of alternating layers of 12 nm Al_2O_3 and 6 nm ZnO. Sample II has exactly the same geometry except the layer thicknesses are doubled to 24 nm (Al_2O_3) and 12 nm (ZnO). Panels d and e in Figure 1 exhibit the result of a TEM-EDX (energy-dispersive X-ray spectroscopy) line scan performed across the cross-section of sample II. It can be clearly seen that abrupt changes occur in the detected Al and Zn levels indicating that the deposited layers have indeed a multilayered sequence with sharp junctions. It is known that the Al_2O_3 films deposited in a wide temperature window by ALD are amorphous. However, ZnO films produced by ALD are always crystalline regardless of the deposition temperature. To investigate the thickness relationship of the ALD-deposited ZnO films with crystalline properties, single-crystal ZnO nanowires were also used as substrates for the ALD deposition of ZnO layers, to

dx.doi.org/10.1021/cm201446y |Chem. Mater. 2011, 23, 4445–4451

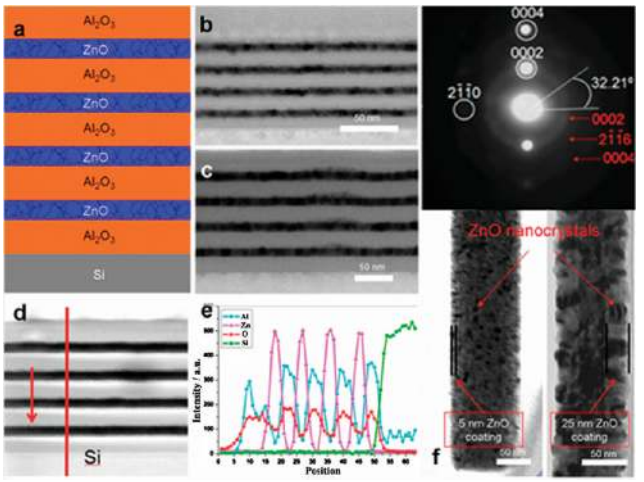

Figure 1. (a) Schematic diagram of multilayered film grown by ALD. Cross-sectional TEM micrographs of (b) sample I consisting of five layers of Al_2O_3 (12 nm, light contrast) and four layers of ZnO (6 nm, dark contrast), and (c) sample II consisting of five layers of Al_2O_3 (24 nm, light contrast) and four layers of ZnO (12 nm, dark contrast). (d) Cross-sectional TEM micrograph of sample II showing the scan line for EDX analysis. (e) EDX results from the line scan shown in d. (f) ZnO nanowires coated with 5 and 25 nm ALD ZnO. Inset is the electron diffraction pattern from the nanowire coated with 5 nm ALD ZnO.

facilitate direct and timely TEM observations. A TEM image of ZnO nanowires coated with a 5 nm ZnO film is displayed in Figure 1f (bottom). The rough surface of the resulting nanowire demonstrates that the ZnO film deposited at a temperature of around 150 °C is actually composed of many tiny crystallites. The top image (Figure 1f) shows the electron diffraction pattern obtained from this nanowire. The simultaneous presence of the indexed diffraction rings confirms the polycrystalline nature of the ALD-deposited ZnO film. When the thickness of the deposited film was increased to 25 nm, larger ZnO crystallites were abundantly formed, as shown in Figure 1f. This result indicates that the crystallite size in the ALD-deposited ZnO films increases with thickness, most possibly due to Ostwald ripening.

Kirkendall Void Formation in the Al_2O_3/ZnO Multilayered Films. For inducing thermal diffusion of the ZnO layers into their adjacent Al_2O_3 layers, both sample I and sample II were annealed at elevated temperatures in air. Figure 2a shows a cross-sectional TEM micrograph of sample I upon annealing at 700 °C for 3 h. It is found that partially continuous nanogaps occurred in place of the original ZnO layers. This process is governed by the reactive Kirkendall-type diffusion of ZnO into Al_2O_3, consistent with our previous results on the formation of spinel $ZnAl_2O_4$ nanotubes by the solid−solid reaction of ZnO−Al_2O_3 core−shell nanowires. However, the nanogaps are not completely continuous even if all the ZnO layers are supposed to be entirely consumed from a chemical viewpoint. The formation of completely continuous nanogaps may have been prevented by the extent of the solid−solid reaction space, which is not confined to a small area as in core−shell nanostructures. Aside from the reaction space, due to dimensions of the deposited thin films, infinitely large and freestanding layers may not be thermally stable as these discrete films would require the means of mechanical support. In the case of ZnO−Al_2O_3 core−shell nanowires, the generated vacancies more easily accumulate and grow into large voids, and finally evolve into nanotubes due to confined reaction space between

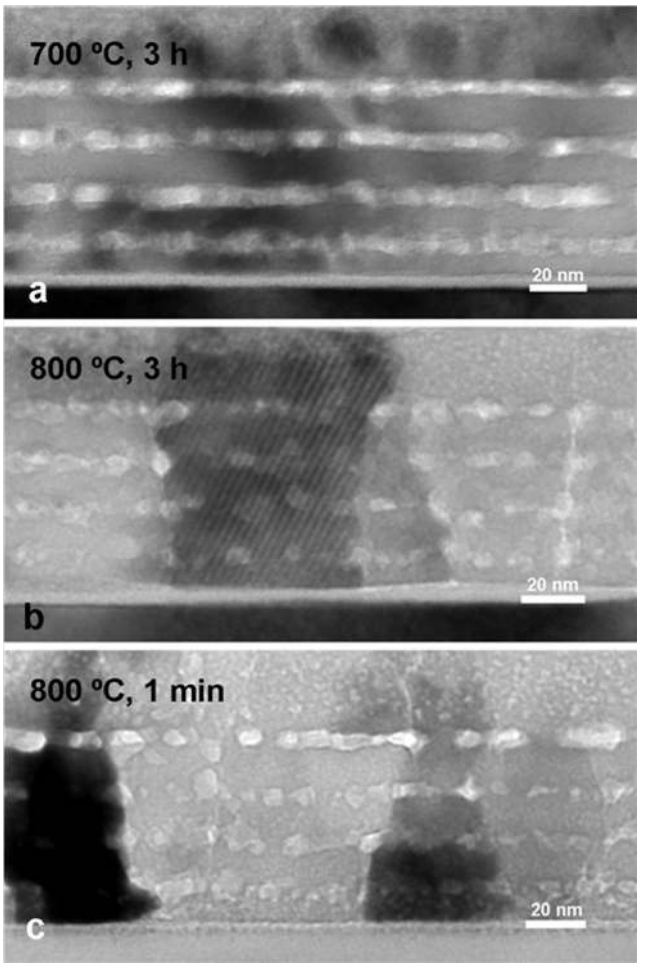

Figure 2. Cross-sectional TEM micrographs of sample I (a) after annealing for 3 h at 700 °C in air, (b) after annealing for 3 h at 800 °C in air, (c) after RTP treatment for 1 min at 800 °C in air.

the reactants as well as the resultant self-supportive tubular structure. When the temperature was raised to 800 °C, the discontinuous morphology feature of the formed nanogaps was amplified and layers of ordered nanocavities appeared (Figure 2b). Especially, the nanocavities seem to have the shape of the initial ZnO nanocrystals, differing from both the interfacial voids evolving by surface diffusion of the Kirkendall voids in the ZnO−Al_2O_3 core−shell nanowires, and those created by the simple decay of the neighboring spinel layers owing to thermal instability.[12] Peng et al. once produced nanolaminate assemblies of Al_2O_3/ZnO/Al_2O_3 trilayers and investigated the bidirectional diffusion of ZnO based on the Kirkendall effect.[20] This study granted that the polycrystalline ZnO thin films behave the same way as single-crystal ZnO substrates during a spinel-forming thermal diffusion process. However, in the current experiments, we demonstrated that the polycrystalline nature of ZnO in the multilayered films cannot be ignored.

In the multilayered films, the polycrystalline ZnO layers introduce many short-circuit diffusion paths via the grain boundary (GB) network.[10] The GBs could easily accommodate diffusion of Al_2O_3 into ZnO layers, since GB diffusivity is much larger than bulk/lattice diffusivity.[21] The preferential GB diffusion of Al_2O_3 causes encapsulation of ZnO crystals, freezing them in their initial positions. Then, the solid−solid $ZnAl_2O_4$-forming reaction

dx.doi.org/10.1021/cm201446y |*Chem. Mater.* 2011, 23, 4445–4451

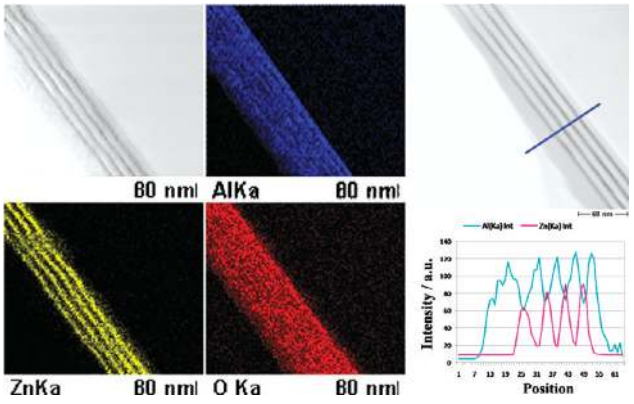

Figure 3. Left: STEM image and corresponding EDX element mappings of Al, Zn, and O for sample I after annealing at 600 °C for 3 h in air. Right: STEM image and intensity profiles of Al and Zn across the multilayer of the same sample.

proceeds between the ZnO grains and the surrounding Al_2O_3. Therefore, when the fast diffuser is altered from monocrystalline to polycrystalline, the diffusion mode shifts from one way diffusion to a concomitant diffusion process where both ZnO and Al_2O_3 diffuse into each other via interfacial bulk ($ZnO \rightarrow Al_2O_3$) and GB diffusion ($Al_2O_3 \rightarrow ZnO$). The GB diffusion of Al_2O_3 into ZnO layers was also confirmed via EDX analysis (Figure 3) on Sample I which was annealed at a lower temperature (600 °C) for 3 h. At this temperature, the spinel forming solid−solid reaction does not easily take place because of insufficient thermal energy. The bulk interface diffusion of ZnO into Al_2O_3 is very slow. Therefore, the presence of Al in the ZnO layers is a direct evidence of the presence of GB diffusion of Al_2O_3. Note that at temperatures ≥700 °C, GB diffusion of Al_2O_3 into ZnO layers and interfacial bulk transfer of ZnO into Al_2O_3 occur simultaneously. Hence, the final void morphology is determined by these two competing processes. Yu et al. studied GB diffusion in the presence of the Kirkendall effect using computer simulations.[22] According to their calculations, in two component systems, GB diffusion is significantly enhanced when vacancies are generated due to the Kirkendall effect. This may be the reason why the GB diffusion becomes even more dominant when the temperature is raised from 700 to 800 °C, as more vacancies are generated at higher temperatures creating a greater GB diffusion component.

For understanding the relationship between the void evolution and the reaction time, annealing of sample I was also performed at 800 °C in air for one minute in a rapid thermal processing (RTP) furnace. As demonstrated by the TEM image shown in Figure 2c, the final Kirkendall void morphology of the RTP sample looks strikingly similar to the results from the sample annealed at 800 °C for three hours. For single-crystal ZnO nanowires coated with an amorphous Al_2O_3 shell, annealing at 800 °C for only 1 min does not result in the formation of many large interfacial voids and complete consumption of the ZnO core is not achieved either. This gives strong evidence that the diffusion of Al_2O_3 along the GBs of ZnO is indeed a kinetically favored process, which significantly increases the interface area between the Al_2O_3 films and the particulate ZnO layers and accordingly accelerates the spinel-forming reaction by the following one-way bulk diffusion of each ZnO nanocrystallite. Therefore, the thermal diffusion and solid-state reaction processes reached equilibrium in a very short time. The high

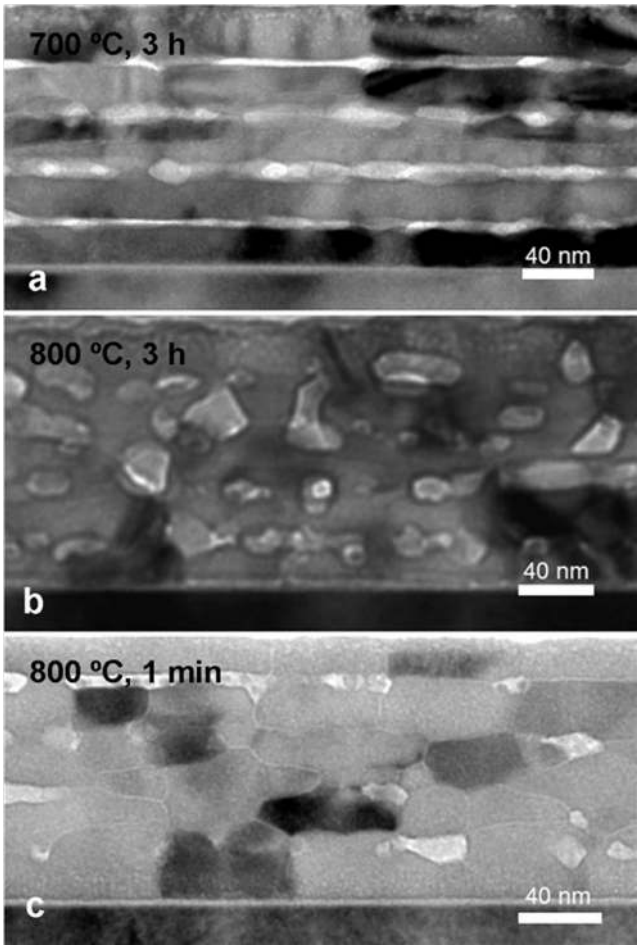

Figure 4. Cross-sectional TEM micrographs of sample II (a) after annealing for 3 h at 700 °C in air, (b) after annealing for 3 h at 800 °C in air, (c) after RTP treatment for 1 min at 800 °C in air.

similarity in the morphology of the samples annealed for 1 min (RTP) and 3 h also confirms that the ordered voids embedded in the multilayered $ZnAl_2O_4$ product derived from sample I is a highly thermally stable configuration. Long-time annealing at 800 °C does not lead to the collapse of the porous structures created by the Kirkendall void formation process.

Next, we investigated the influence of layer thickness on the Kirkendall void morphology in the multilayered films. As shown in Figure 1f, an increased layer thickness is directly associated with increased ZnO grain size, which has been proved to greatly affect the GB diffusion process. The effective solute diffusion in polycrystalline solids can be described by the general Hart-Mortlock equation as shown below[23]

$$D_{\mathrm{Eff}}(\mathrm{Hart-Mortlock}) = sgD_{\mathrm{GB}} + (1 - sg)D_{\mathrm{L}} \quad (1)$$

Here, D_{Eff} is the effective diffusivity, s the segregation factor, g the volume fraction of atomic sites in the GB of the polycrystal, D_{GB} the GB diffusivity, and D_{L} the lattice (i.e., bulk) diffusivity. The term g can be written as $g = (q\delta)/(d)$, where q is a grain shape-dependent numerical factor ($q = 1$ for parallel grains), δ the GB width (treated as constant ~0.5 nm), and d is the grain size. According to this equation, the GB diffusion of Al_2O_3 into ZnO should be reduced with increasing ZnO grain size d. Hence, multilayered films with bigger ZnO crystals (sample II) should

dx.doi.org/10.1021/cm201446y |*Chem. Mater.* 2011, 23, 4445–4451

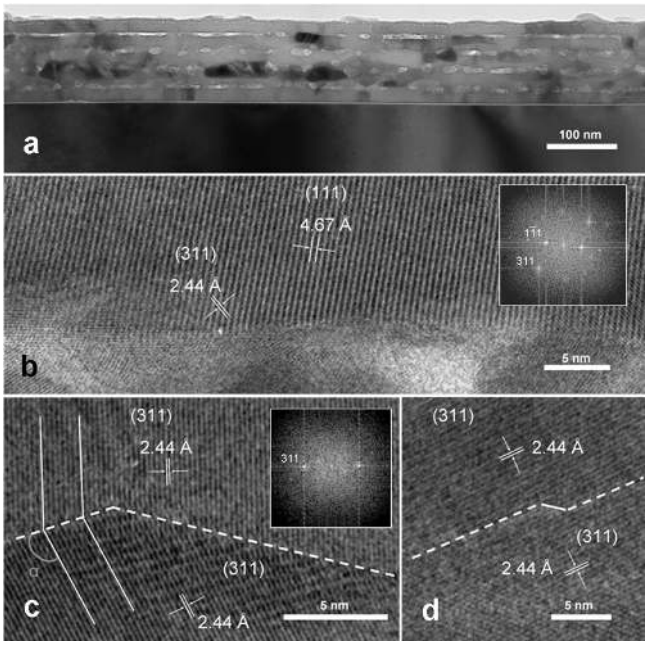

Figure 5. (a) Low-magnification TEM image of sample II annealed for 1 min at 800 °C in air. High-resolution TEM micrographs of (b) top $ZnAl_2O_4$ spinel layer, (c) adjacent bicrystals attached with an angle α, (d) adjacent bicrystals attached without an angle. Note that dashed lines are the grain boundaries.

show a better gap profile than sample I at lower temperatures such as 700 °C because the increased grain size of ZnO can reduce the GB diffusion of Al_2O_3.

To confirm these assumptions, sample II was subjected to the same thermal processes as sample I. First, sample II was annealed at 700 °C for 3 h. The resulting pore morphology is shown in Figure 4a. Under these annealing conditions, long and partially segmented nanogaps were formed. The pore morphology resembles the results obtained from sample I at 700 °C but this time the gaps seem to have a more continuous profile. When the thermal process was repeated at 800 °C for 3 h, the multilayered film unexpectedly transformed into a $ZnAl_2O_4$ film with a random, unordered pore morphology with unexpectedly large cavities as shown in Figure 4b. To understand the source of the large voids and the random pore morphology, sample II was also subjected to a 1 min RTP anneal in air at 800 °C. The resulting structure, see Figure 4c, is an intermediate, nonequilibrium stage in the thermal process, where large spinel crystals are clearly visible. The formation of large spinel crystals during the solid−solid reaction is not surprising due to the larger size of the initial ZnO crystals in sample II. It appears that the formed voids travel through the $ZnAl_2O_4$ GB network, settle and enlarge in energetically favorable sinks, which leads to formation of large interlaced voids in the film. Although increased grain size of ZnO reduces the influence of Al_2O_3 GB diffusion into the ZnO layers, the ordered gap morphology decayed at higher temperatures such as 800 °C because of lower porosity and enhanced GB migration of the formed $ZnAl_2O_4$.[10]

Figure 5 shows a series of high-resolution TEM (HRTEM) images of sample II after the RTP treatment at 800 °C. Figure 5a represents a low-magnification TEM micrograph belonging to this sample. Various sites are selected from this sample for HRTEM analysis to determine the underlying cause of the randomly ordered void morphology. Interestingly, even though the sample consists of randomly ordered large voids, relatively long, partially continuous gap formations are visible beneath the top layer. This is also the case for sample I thermally treated by RTP at 800 °C for 1 min. The HRTEM micrograph in Figure 5b demonstrates that the top first layer is composed of long-sectional monocrystalline $ZnAl_2O_4$. The distinctive gap-like morphology under this $ZnAl_2O_4$ cap indicates that the diffusion behavior of the ZnO top layer is different from that of the other layers. It is reasonable to consider that the sandwiched ZnO top layer is not really embedded during the RTP-induced solid−solid reaction because the stress-induced cracks in the top Al_2O_3 layer can facilitate its outward diffusion/evaporation into the air.[13] Figure 5c shows two large adjacent $ZnAl_2O_4$ bicrystals located inside the multilayered film. The crystals are attached to one another with a small angle α with the same crystal facets facing each other. This result suggests that large crystals in the $ZnAl_2O_4$ film having clear facets can approach, attach, and fuse each other in an oriented manner during thermal annealing at higher temperatures.[24] The GB migration of the formed $ZnAl_2O_4$ domains could be triggered and enhanced by the increased mechanical stress within the multilayered film due to larger overall film thickness and lower porosity due to increased ZnO grain size.[10,25] Moreover, large nanocrystallites are known to be better faceted than small ones. For instance, very small Au nanocrystals are approximately spherical in shape, forming no clear facets but this is not the case when the crystal size is increased. Thus, when sample I was annealed under the same conditions as sample II, ordered void morphology was retained as a result of smaller overall multilayered film thickness and higher porosity which prevented major GB migration. Additionally, large spinel grains forming across the multilayer stack were occasionally observed in sample I after annealing at 800 °C, as shown in Figure 2b. These large crystals were most probably produced by the fusion of small immobile adjacent grains annealed at such a high temperature. The ordered void morphology in the multilayer stack is not disturbed in the presence of these large crystals, suggesting the absence of major grain boundary migration during the reaction. In contrast, these reconfiguration processes became severe and widespread when the film thickness and ZnO grain size were increased (sample II). Figure 5d shows bicrystals that are again attached in an oriented manner. Because this time the attachment angle is zero and the grains are well-aligned, if annealed further, these crystals will most likely fuse and grow into a bigger crystal.[26]

A schematic summary of the Kirkendall void development in our multilayered films is presented in Figure 6. The overall void evolution can be considered as a two stage process (Figure 6a). In the first stage, Al_2O_3 diffuses into ZnO via GBs surrounding the ZnO nanocrystals in the layers. In the second stage, ZnO diffuses into the surrounding Al_2O_3 through the interface via bulk diffusion which results in inward injection of vacancies and formation of embedded ordered Kirkendall voids. If the initial ZnO layers in the multilayered film are thick, the GB diffusion of Al_2O_3 into ZnO is partially weakened because of increased grain size. Better gaplike layered nanostructures are formed, accompanying the formation of large $ZnAl_2O_4$ crystals. However, increased mechanical stress, reduced porosity, and well-faceted crystallite morphology in this case very easily initiate GB migration of the formed $ZnAl_2O_4$ crystals at higher temperatures and lead to degradation of the layered structures. Such a structural development process is schemed in Figure 6b.

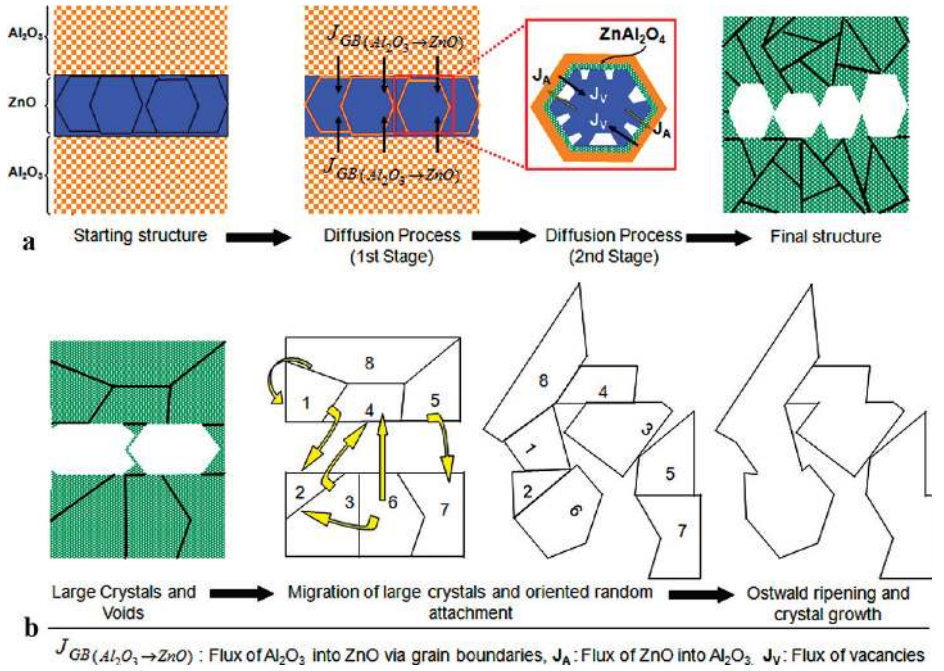

Figure 6. Schematic illustration of (a) Kirkendall void development in Al_2O_3/ZnO multilayered films containing polycrystalline ZnO layers, (b) oriented attachment of large $ZnAl_2O_4$ crystals and crystal growth via Ostwald ripening.

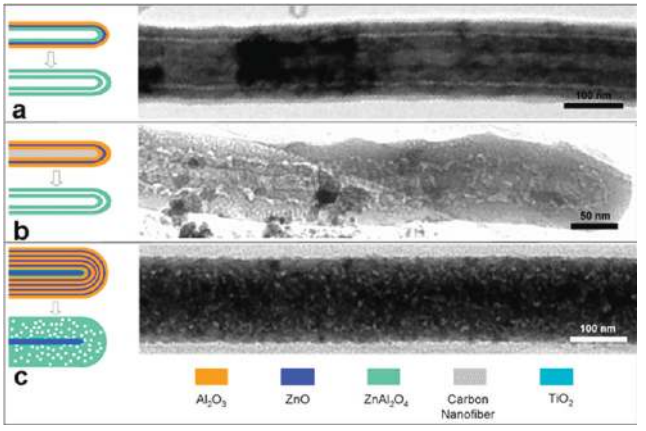

Figure 7. Nanostructures coated with multilayered films illustrated schematically before and after annealing (left) along with a TEM micrograph after annealing (right): (a) $ZnAl_2O_4$ nanotube coated with a single pair of ZnO and Al_2O_3 annealed at 700 °C. (b) Carbon nanofiber coated with a multilayered film with three alternating layers of Al_2O_3 and ZnO annealed at 700 °C. (c) ZnO nanowire coated with a multilayered film with nine alternating layers of Al_2O_3 and ZnO annealed at 800 °C.

Design of 1D Porous Nanostructures Using Multilayered Films. Knowledge on void formation by the Kirkendall effect as obtained from thin-film diffusion couples can be directly applied to the design of hollow nanostructures. Based on the above investigations, the arrangement of the Kirkendall void morphology in multilayered films is further explored to create complex 1D porous nanostructures starting from 1D templates shelled by the Al_2O_3/ZnO multilayered films. More importantly, the influence of reaction temperature and layer thickness on the morphology of the final products known from the Al_2O_3/ZnO multilayered films can be profitably referred. In the following case experiments, the thicknesses of ZnO (12 nm) and Al_2O_3 (24 nm) layers are employed, consistent with the layer thicknesses in sample II. The first example schematically shown in the left of Figure 7a involves a single-crystal $ZnAl_2O_4$ nanotube coated with a single pair of ZnO and Al_2O_3. Here, the nanotube acts as an inert 1D template. After this sample was annealed at 700 °C for 3 h, ordered pore/channel formation in place of the former ZnO layer is visible, producing a so-called tube-in-tube structure (right TEM image of Figure 7a). Because only one side of the ZnO layer is coated by the Al_2O_3 film, it can be expected that the GB diffusion of Al_2O_3 into the ZnO layer is approximately reduced by half in this case. Besides, the stress-induced cracks in the outer Al_2O_3 layer can facilitate the outward diffusion/evaporation of the ZnO layer into the air, as we mentioned before. Therefore, the formed hollow space presents a continuous gaplike morphology feature. When an Al_2O_3/ZnO/Al_2O_3 trilayer was coated on a carbon nanofiber template (see Figure 7b), this system was again transferred to the tube-in-tube structure after annealing at 700 °C with the template combusted in air. However, compared with the structure shown in Figure 7a, a more granular void distribution appears between the outer and inner nanotube. This result is reasonable because the GB diffusion of Al_2O_3 is more obvious for a ZnO layer sandwiched by amorphous Al_2O_3 films, which more easily leads to "faceted" voids. Finally, we performed an experiment with our nine layered film coated on a 1D template (ZnO nanowires protected by a TiO_2 diffusion barrier shell) at 800 °C. As expected, the multilayered shell was transformed into porous $ZnAl_2O_4$ nanostructures with unordered pores (Figure 7c). This suggests that the GB migration of the formed relatively large $ZnAl_2O_4$ domains at 800 °C makes this system thermally unstable, in agreement with the result obtained from the multilayered film shown in Figure 4b.

CONCLUSIONS

We studied the morphology development of Kirkendall voids in ALD-grown Al_2O_3/ZnO multilayered films. The alternating

dx.doi.org/10.1021/cm201446y |*Chem. Mater.* 2011, 23, 4445–4451

stack of amorphous Al_2O_3 and polycrystalline ZnO layers provides a representative example for investigating the Kirkendall void formation in a polycrystalline infinite space. The effects of annealing temperature, grain size, reaction time and reaction space on the void features of final spinel products are studied in detail. It is found that more GBs existing in thin ZnO layers significantly enhance the GB diffusion of Al_2O_3 into the ZnO layers at 700 °C. The resultant $ZnAl_2O_4$ multilayer represents ordered voids in the original positions of the ZnO layers, exploiting the following one-way diffusion of ZnO into the surrounding Al_2O_3. This porous structure is rigid at higher reaction temperature such as 800 °C because of the restricted GB migration of small $ZnAl_2O_4$ crystallites formed under this condition. The employment of thick ZnO layers (reduced GBs) favors the creation of large gaps in the multilayered spinel nanostructures as a result of the reduced GB diffusion of Al_2O_3 into the ZnO layers. However, the produced structure is easy to decay at higher temperatures due to enhanced GB migration of the formed big $ZnAl_2O_4$ crystallites. We have also established models for the development of voids with different processing conditions. It should be mentioned that the reaction product spinel $ZnAl_2O_4$ had been shown to be an important material in tissue engineering, optical, photo, and electroluminescence applications as well as catalytic applications. Controlled regulation of the void features in this material will largely enrich its functionalities in various areas. The results presented here should allow synthesis of new multilayered nanostructures with controlled pore morphologies and can be extended to other Kirkendall-type thermal diffusion couples.

AUTHOR INFORMATION

Corresponding Author

*E-mail: gueder@imtek.de (F.G.); yang.yang@imtek.de (Y.Y.).

ACKNOWLEDGMENT

This work was supported by Deutsche Forschungsgemeinschaft (DFG) under contracts ZA 131/23-1 (Freiburg) and HE 2100/8-1 (Halle).

REFERENCES

(1) Smigelskas, A. D.; Kirkendall, E. O. *Trans. AIME* **1947**, *171*, 130.
(2) Yin, Y.; Rioux, R. M.; Erdonmez, C. K.; Hughes, S.; Somorjai, G. A.; Alivisatos, A. P. *Science* **2004**, *304*, 711.
(3) Wang, Y.; Cai, L.; Xia, Y. *Adv. Mater.* **2005**, *17*, 473.
(4) Fan, H. J.; Knez, M.; Scholz, R.; Nielsch, K.; Pippel, E.; Hesse, D.; Zacharias, M.; Gösele, U. *Nat. Mater.* **2006**, *5*, 627–631.
(5) Fan, H. J.; Gösele, U.; Zacharias, M. *Small* **2007**, *3*, 1660.
(6) Yang, Y.; Kim, D. S.; Scholz, R.; Knez, M.; Lee, S. M.; Gösele, U.; Zacharias, M. *Chem. Mater.* **2008**, *20*, 3487.
(7) An, K.; Hyeon, T. *Nano Today* **2009**, *4*, 359.
(8) Cabot, A; Smith, R. K; Yin, Y; Zheng, H; Reinhard, B. M.; Liu, H.; Alivisatos, A. P. *ACS Nano* **2008**, *2*, 1452.
(9) Cabot, A; Ibanez, M; Guardia, P; Alivisatos, A. P. *J. Am. Chem. Soc.* **2009**, *131*, 11326.
(10) Kaganovskii, Yu.; Paritskaya, L. N. Diffusion in Nanomaterials. In *Encyclopedia of Nanoscience and Nanotechnology*; American Scientific Publishers: Valencia, CA, 2004; Vol. 2, p 399.
(11) Fan, H. J.; Knez, M.; Scholz, R.; Hesse, D.; Nielsch, K.; Zacharias, M.; Gösele, U. *Nano Lett.* **2007**, *7*, 993.
(12) Yang, Y.; Kim, D. S.; Knez, M.; Scholz, R.; Berger, A.; Pippel, E.; Hesse, D.; Gösele, U.; Zacharias, M. *J. Phys. Chem. C* **2008**, *112*, 4068.
(13) Güder, F.; Yang, Y.; Goetze, S.; Berger, A.; Ramgir, N.; Hesse, D.; Zacharias, M. *Small* **2010**, *6*, 1603.
(14) Yang, Y.; Güder, F.; Zacharias, M. *Isr. J. Chem.* **2010**, *50*, 439.
(15) Kim, H. *J. Vac. Sci. Technol. B* **2003**, *21*, 2231.
(16) Puurunen, R. J. *J. Appl. Phys.* **2005**, *97*, 121301.
(17) Knez, M.; Niesch, K.; Niinistö, L. *Adv. Mater.* **2007**, *19*, 3425.
(18) Güder, F.; Yang, Y.; Krüger, M.; Stevens, G. B.; Zacharias, M. *ACS Appl. Mater. & Interf.* **2010**, *2*, 3473.
(19) Zhang, L.; Jiang, H. C.; Liu, C.; Dong, J. W.; Chow, P. *J. Phys. D: Appl. Phys.* **2007**, *40*, 3707.
(20) Peng, Q.; Sun, X.-Y.; Spagnola, J. C.; Saquing, C.; Khan, S. A.; Spontak, R. J.; Parsons, G. N. *ACS Nano* **2009**, *3*, 546.
(21) Shewmon, P. *Diffusion in Solids*, 2nd ed.; The Minerals, Metals and Materials Society: Warrendale, PA, 1989; p 191.
(22) Yu, H. C.; Van der Ven, A.; Thornton, K. *Appl. Phys. Lett.* **2008**, *93*, 091908.
(23) Mehrer, H. *Diffusion in Solids: Fundamentals, Methods, Materials, Diffusion-Controlled Processes*; Springer: New York, 2007; p 569.
(24) Penn, R. L.; Banfield, J. F. *Science* **1998**, *281*, 969.
(25) Rupert, T. J.; Gianola, D. S.; Gan, Y.; Hemker, K. J. *Science* **2009**, *326*, 1686.
(26) Yang, Y.; Scholz, R.; Fan, H. J.; Hesse, D.; Gösele, U.; Zacharias, M. *ACS Nano* **2009**, *3*, 555.